

# Sensing Performance of the IEEE 802.11bf Protocol and Its Impact on Data Communication

Anirudha Sahoo<sup>1</sup>, Tanguy Ropitault<sup>2,3</sup>, Steve Blandino<sup>2,3</sup> and Nada Golmie<sup>1</sup>

<sup>1</sup>National Institute of Standards and Technology, Gaithersburg, Maryland, USA

<sup>2</sup>Associate, National Institute of Standards and Technology, Gaithersburg, Maryland, USA

<sup>3</sup>Prometheus Computing LLC, Bethesda, Maryland, USA

Email: {anirud, tanguy.ropitault, steve.blandino, nada}@nist.gov

**Abstract**—Wi-Fi sensing has been used to detect and track movements in an environment, resulting in the emergence of several innovative applications. Wi-Fi sensing can detect movement and locate objects by analyzing variations in the Wi-Fi signal due to its interaction with moving objects. Until recently, Wi-Fi sensing has been primarily available through proprietary solutions, which has limited its adoption. However, the recent initiative by the IEEE to develop the IEEE 802.11bf standard promises to make the adoption of Wi-Fi sensing widespread. Although Wi-Fi sensing procedures in communication standards can be overhead, there is currently a lack of literature exploring the sensing performance of Wi-Fi sensing procedures specified in the IEEE 802.11bf standard and its impact on data communication. Therefore, this paper presents a comprehensive evaluation of the sensing performance of the IEEE 802.11bf protocol and its impact on data communication in different configurations. Our findings expose the limitations of specific configurations and pave the way to provide guidance on efficient operating configurations of an IEEE 802.11bf network.

## I. INTRODUCTION

Using Wi-Fi sensing, changes in the Wi-Fi radio channel can be used to detect movements in the environment, enabling a wide range of applications such as presence of humans, localization, fall detection, etc. [1]. Since Wi-Fi networks are widely deployed, the above paradigm would make it possible to make aforementioned diverse set of applications available to the users and eliminate the need for different kinds of sensors for different applications. Although a lot of work has been reported in the literature about Wi-Fi based sensing [1]–[8], lack of standardization has limited the proliferation of Wi-Fi sensing based applications. Therefore, the Task Group IEEE 802.11bf (TGbf) started the development of an amendment to the IEEE 802.11 standard in September 2020 to standardize Wi-Fi based sensing [9] which will be known as IEEE 802.11bf. The IEEE 802.11bf standard defines Wireless Local Area Network (WLAN) sensing procedures, both in the sub-7 GHz [9], [10] and above 45 GHz band [9], [11].

Integrating sensing with data communication in Wi-Fi network is quite attractive since it allows for more efficient use of spectrum and hardware. However, for sensing, the system generally needs to allocate a part of its radio resources to send dedicated sounding frames and other sensing related information, reducing resources available for regular data communication. Thus, sensing becomes an overhead for data communication. There is no study that quantifies the impact

of implementing Wi-Fi sensing procedures, specified in the IEEE 802.11bf standard, on data communication. In this work, we implement the most recent features of the IEEE 802.11bf protocol in the sub-7 GHz band by extending the *IEEE 802.11ax lightsim software* [12] and conduct a thorough assessment of WLAN sensing performance as well as its impact on data communication. Given the novelty of a Wi-Fi network performing sensing procedures, we also introduce new performance metrics, which are designed to quantify both the overhead introduced by the sensing procedures and the failure rate of the sensing operations.

In the IEEE 802.11bf sensing protocol for sub-7 GHz, the actual sensing measurements are done during, what are called, *sensing measurement exchanges* (SMEs), and those SMEs account for most of the sensing overhead. So, in this study, we focus on the SME part of the protocol. To perform an SME, the initiator of sensing, which could be the Access Point (AP) or a Wi-Fi Station (STA), has to get access to the channel and obtain a Transmission Opportunity (TxOP). It may use Enhanced Distributed Channel Access (EDCA) or Point coordination function (PCF) Interframe Space (PIFS) to get a TxOP. The IEEE 802.11bf protocol also defines a periodically occurring sensing window, within which the SMEs have to be performed. The duration and periods of sensing windows are configurable. We examine both the EDCA and PIFS based access methods at different sensing loads in the system when the AP is the initiator of sensing. We present extensive simulation results at different system configurations corresponding to different sensing loads. Our simulation results have uncovered significant findings that will facilitate the efficient configurations of future IEEE 802.11bf systems operating in the sub-7 GHz band.

The main contributions of this work are as follows.

- To the best of our knowledge, this is the first work to present an extensive simulation of the IEEE 802.11bf protocol.
- This work provides quantitative insights into the sensing performance of the IEEE 802.11bf protocol and its impact on data communication in terms of the defined performance metrics.
- Our simulation exposes the limitations of WLAN sensing using EDCA based access when sensing reports need to be sent from sensing STAs to the AP.
- The results presented in this work provide guidance and insights into efficient operating configurations of an IEEE

## II. RELATED WORK

There has been a lot of research work on Wi-Fi sensing reported in the literature. In [3], the authors present a passive Wi-Fi radar system for human sensing by exploiting high data rate OFDM signals and periodic Wi-Fi beacon signals. Change in Received Signal Strength (RSS) in a commercial off-the-shelf (COTS) Wi-Fi device held on a person's chest is used to design a respiratory monitoring system in [2]. Changes in Wi-Fi signal strength have been studied to detect hand gestures around a user's mobile device in [4]. In [6], the authors have implemented an end-to-end system to monitor human respiratory motion using Wi-Fi Channel State Information (CSI). They propose a deep learning based processing algorithm called *BreatheSmart* that analyzes the changes in amplitude and phase of CSI data to detect respiratory motion. In [7], a four antenna passive bistatic indoor radar configuration is set up using IEEE 802.11ax Wi-Fi system to track multi-target human based on range, doppler and angle-of-arrival measurements. A prototype of Wi-Fi based passive radar system for localization and tracking of moving targets using range, doppler and direction of arrival is presented in [8]. The above mentioned research works are focused on methodologies or algorithms for the concerned applications, but do not deal with estimating the Wi-Fi sensing related overhead of the system. A fairly comprehensive survey of Wi-Fi sensing with CSI is presented in [1].

To standardize Wi-Fi sensing process, the TGBf is developing a standard which will be known as IEEE 802.11bf [9]. This standard defines the mechanisms and protocols to provide channel state information in the sub-7 GHz band and radar based information (e.g., range, doppler, beam azimuth) above the 45 GHz band. Since Wi-Fi sensing protocol is an overhead to the Wi-Fi data communication, it is important to study the performance of Wi-Fi sensing and its impact on data communication in different configurations. To the best of our knowledge, there is no such study available in the literature.

## III. OVERVIEW OF IEEE 802.11BF SENSING PROCEDURE

An IEEE 802.11bf capable STA and AP exchange their sensing capabilities during the association process. WLAN sensing in the sub-7 GHz band, referred to as *Sensing Procedure*, starts out with the establishment of a *sensing measurement session* between a *sensing initiator* and a *sensing responder* at which time the operating parameters of the session are determined. Examples of operating parameters include bandwidth, the role of the STAs (sensing transmitter or sensing receiver), timer values etc. The actual sensing measurements are performed in SMEs. SMEs can be trigger based (TB) or non-trigger based (NTB). Since TB SME is envisioned to be the most common deployment scenario, we focus on TB SME in this study. In a TB SME, an AP is the sensing initiator and one or more non-AP STAs are the sensing responders. An AP starts a TB SME by obtaining a TxOP after a *sensing availability window* (SAW) period starts. A SAW has two parameters: *SAW duration* and *SAW period*. SAW durations

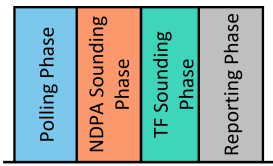


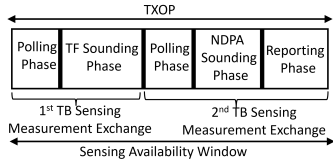
Fig. 1: Different phases in a TB Sensing Measurement Exchange

occur periodically and their periods are determined by the SAW period parameter. An AP and the STAs may participate in SMEs only in a SAW duration. A TB SME can have up to four phases as shown in Fig. 1. In the polling phase, an AP (the sensing initiator) sends a Sensing Polling Trigger frame to the sensing responder STAs inviting them to participate in the SME. In the Null Data Packet Announcement (NDPA) Sounding phase the AP is the sensing transmitter and one or more STAs are the sensing receivers. The AP sends an NDPA frame followed by a Null Data Packet (NDP) frame to the receiver STAs. The STAs measure the channel state using the received NDP frame. In the Trigger Frame (TF) Sounding phase, the AP acts as the sensing receiver and the STAs as sensing transmitters. The AP sends a TF to the sensing receiver STAs, which then send NDP frames (which are multiplexed in the spatial domain) to the AP. The AP measures the channel state using the received NDP frames. The reporting phase is present, if sensing report (mainly consisting of CSI) is required to be sent from the STAs to the AP. Orthogonal Frequency Division Multiple Access (OFDMA) mechanism is used for reporting, for which the AP allocates Resource Units (RUs) to the STAs. Only the NDPA sounding phase may necessitate a Reporting phase, if reporting was enabled as part of operational parameters during the sensing measurement session setup. For more details on TB SME, please refer to [9].

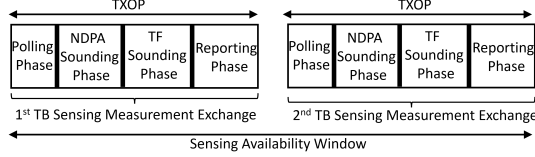
As mentioned earlier, an AP performs TB SMEs within a TxOP, after obtaining the TxOP within a SAW. A SAW may contain a single TxOP (Fig. 2a) or more than one TxOP (Fig. 2b). An AP may obtain the TxOP by EDCA or PIFS mechanism. We refer to them as *EDCA access* and *PIFS access* respectively. If it uses EDCA access, then due to contention, the actual SAW duration available for SMEs sometimes may be shorter than the configured SAW duration. But when PIFS access is used, AP gets priority access to the channel and hence, gets almost the entire SAW duration for sensing.

### A. Overhead Calculation

The Sensing Procedure is an overhead for data communication. The majority of the overhead is incurred in the SME part of the protocol. So, in this study, we concentrate on the SME part of the protocol. In an SME, the NDPA sounding phase and Reporting phase account for most of the overhead. Hence, our overhead calculation involves only those two phases. Note that in an NDPA sounding phase, the AP acts as a sensing transmitter, and one or more STAs act as sensing receivers. For the NDPA sounding phase, we take the number of bytes in NDPA and NDP frame structure as overhead [9]. The NDPA



(a) SAW with two SMEs within a single TxOP



(b) SAW Spanning across two TxOPs, each with an SME  
Fig. 2: Illustration of SAW, TxOP and SMEs

frame structure is presented in Fig. 9.58 in [13] and the STA Info field format used in the NDPA frame is shown in Fig. 9-61da in [14]. The NDP format shown in Fig. 27.46a in [14] is used for the computation of NDP overhead. For the reporting overhead, we use the CSI size computation used in Equation (9-5f) in [9]:

$$CSI \text{ size} = \lceil 1.5 \times N_{tx} \times N_{rx} \rceil + \frac{N_{tx} \times N_{rx} \times N_b \times N_{sc}}{4} + 2 \times N_{rx}, \quad (1)$$

where  $N_{tx}$  is the number of transmit antennas,  $N_{rx}$  is the number of receive antennas,  $N_b$  is the number of bits used for quantization of each CSI value,  $N_{sc}$  is the number of subcarriers reported in CSI. The bytes transmitted as part of NDPA, NDP, and reporting frame will be referred to by a general term called *sensing information bytes* throughout this paper.

#### IV. SIMULATION EXPERIMENTS

##### A. Simulation Setup

In our simulation setup, in terms of network topology, we assume that there is one AP and a variable number of STAs associated with the AP. Our simulation assumes that all messages are received correctly by the receiver, i.e., there is no message error due to interference.

We assume that each sensing application runs on every STA in the network and that the AP requires CSI report from every STA in the network for a given sensing application. Due to resource limitations, if a complete report cannot be sent from a STA, the STA still sends a partial report. Although this will not happen in practice, we resort to this method to highlight the sensing overhead and the missed sensing that such cases lead to. When there is no sensing activity in the network, the STAs send data traffic using EDCA with full bandwidth. We assume that each STA always has at least a TxOP worth of data to send. The TxOP duration was set to its maximum value of 5.484 ms [15]. The AP only participates in sensing and does not send any data traffic.

Since the SME part of the Sensing Procedure incurs the most overhead, this has the most impact on data communication. Hence, it is the focus of our simulation. As mentioned in

Section III-A, we compute overhead based on the NDPA sounding and Reporting phase of an SME. During the Reporting phase, the AP allocates one RU (RU sizes given in Table I) to each STA, which is used by each STA to send sensing reports using OFDMA. We have developed our simulator by extending the *lightsim* software, which was used in the simulation study reported in [15], with IEEE 802.11bf features [12].

TABLE I: Subcarrier Allocation vs. Number of STAs

Number of STA	Subcarriers per STA (size of RU allocation per STA)
1	996
2	484
[3 - 4]	242
[5 - 9]	106
[10 - 16]	52

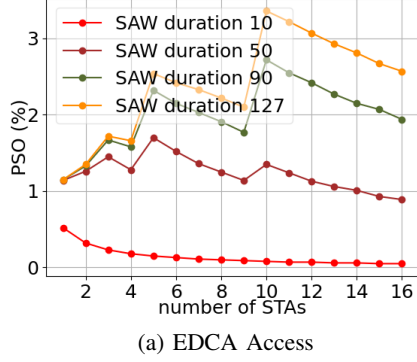
##### B. Performance Metrics

Since this is the first work that evaluates the performance of the IEEE 802.11bf protocol, no pre-existing performance metrics are available for this study. Hence, we define the following performance metrics.

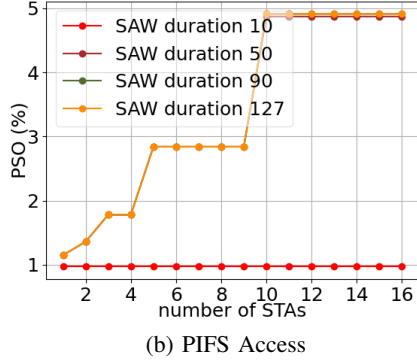
- Percentage Sensing Overhead (PSO): It is the percentage of total simulation duration spent on exchanging sensing information bytes.
- Percentage Sensing Missed (PSM): In every SAW period, sensing is considered to be complete, if all the sensing information bytes for all the applications are able to be sent in the SAW duration. If no sensing messages were sent (completely missed) or only a part of sensing messages were sent (partially missed), then we consider those cases as *sensing missed*. So, the percentage of the number of SAW periods in which sensing is missed is defined as Percentage Sensing Missed (PSM).
- Data Throughput: This is the total number of data bits sent by all the STAs divided by the simulation time.
- Percent Available Window Duration (PAWD): This is defined as the percentage of SAW duration actually available for sensing related tasks. Note that when EDCA access is used, some part of the SAW duration may be lost due to contention. The PAWD would fall below 100% in such situations.

##### C. Simulation Experiment Design

Three parameters decide the sensing load in an IEEE 802.11bf network: (i) the number of sensing STAs, (ii) the number of sensing applications, and (iii) the number of transmit and receive antennae involved in sensing. Hence, for this study, we increased the sensing load in the system by increasing the value of one of those parameters while keeping the values of the other two constant. This led us to run our experiments in three configurations. However, due to space limitation, we are not able to present the results of the third configuration in



(a) EDCA Access



(b) PIFS Access

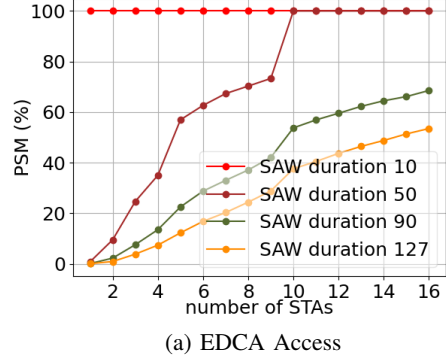
Fig. 3: Sensing Overhead vs number of STAs (Configuration 1)

TABLE II: Simulation Parameters Common to all Configurations

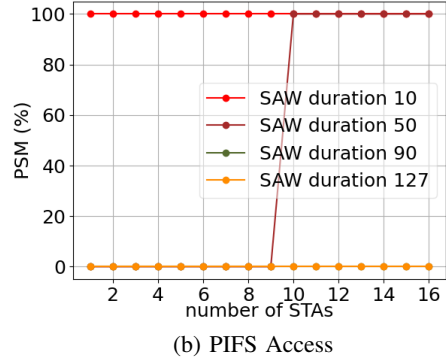
Parameter	Value
Sensing availability window period	1 (=100 TU = 102.4 ms)
TxOP duration	5.484 ms
Number of antennas in the AP	8
Number of antennas in each STA	2
AP Bandwidth	80 MHz
STA Bandwidth	80 MHz
maximum number of subcarriers	996
subcarrier grouping ( $N_g$ )	4
Number of subcarriers reported in CSI ( $N_{sc}$ )	250
Number of bits used for quantization of each CSI value ( $N_b$ )	8
EDCA transmission in a TxOP	Payload = 10 ethernet packets of size 1500 bytes each in an A-MPDU
MCS	6
Simulation duration	10000 seconds

which sensing load was increased by increasing the number of transmit and receive antennae. The two configurations presented in this paper are described below.

- Configuration 1: In this configuration, sensing load is increased by increasing the number of STAs ( $nSTA$ ) involved in sensing at different SAW durations. The number of applications is fixed at 4, and the sensing transmitter and receiver antenna configuration is set to 2x2. Note that sensing transmitter and receiver antenna configuration 2x2 implies that for each STA, the AP



(a) EDCA Access



(b) PIFS Access

Fig. 4: Missed Sensing vs. number of STAs (Configuration 1)

(sensing transmitter) uses two of its eight antennae, and each STA (sensing receiver) uses all of its two antennae. Thus, the AP can engage with up to four STAs in an SME for sensing.

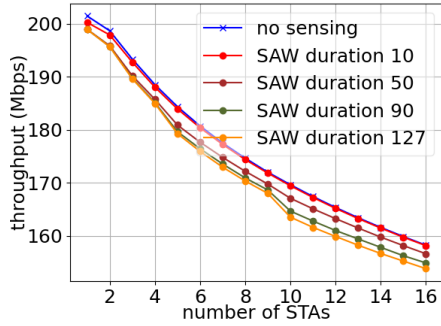
- Configuration 2: Sensing load, in this configuration, is increased by increasing the number of sensing applications ( $numApp$ ) in the system at different  $nSTA$  values. The SAW duration is fixed at 127 (Note: SAW duration 1 = 100  $\mu$ s), which corresponds to its maximum possible value of 12.7 ms. The sensing transmitter and receiver antenna configuration is set to 2x2.

Simulation parameters common to all configurations are shown in Table II.

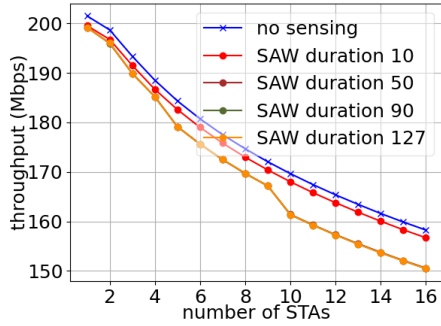
#### D. Experiment Results

1) Configuration 1: Fig. 3a shows how PSO changes as  $nSTA$  increases with EDCA access. Generally, PSO decreases as  $nSTA$  increases, because there is more contention for getting TxOP for sensing, and hence, less duration is available for sensing. However, PSO increases from  $nSTA = 4$  to 5 and from  $nSTA = 9$  to 10 for SAW duration  $> 10$ . At these  $nSTA$  transition points, the size of an RU assigned to each STA goes down (see Table I). Hence, more time is needed to send a given number of sensing information bytes, thereby increasing the overhead. SAW duration 10 (1 ms) is very short relative to the SAW period of 102.4 ms. Hence, the overhead is very low in this case, and at high  $nSTA$ , due to high contention, PSO goes down to almost zero.

As seen in Fig. 3b, with PIFS access, PSO remains unchanged when RU size per STA does not change. Unlike



(a) EDCA Access



(b) PIFS Access

Fig. 5: Throughput vs. number of STAs (Configuration 1)

EDCA access, there is no variability in actual SAW duration available for sensing since no contention is involved. Report size per STA does not change since the number of applications is constant in this configuration. Hence, PSO remains constant in the intervals where RU size per STA does not change. But when RU size per STA decreases (e.g., from  $nSTA = 9$  to 10), the duration to send sensing report goes up, and hence, PSO goes up. SAW duration = 10 is too short, which limits the number of sensing information bytes sent to a constant value across the  $nSTA$  values, and hence, PSO does not change. Note that PSO for SAW durations 90 and 127 are identical all throughout. For these two SAW durations PSM is 0% all throughout (see Fig. 4b). Hence, the amount of sensing information bytes sent is the same for the two SAW durations. For SAW duration 50, PSO is identical to those of SAW duration 90 and 127 until  $nSTA=9$ , since PSM is 0% until that point. But after that, PSM goes up to 100%. But these missed sensing are due to partial missed sensing, and PSO beyond  $nSTA=9$  is just 0.04% lower than those of SAW durations 90 and 127. Hence, its PSO looks almost identical to them after  $nSTA=9$ . This indicates that SAW duration 50 fell slightly short of the duration needed to send all the sensing information bytes.

With EDCA access, as  $nSTA$  increases, PSM increases (see Fig. 4a). Due to more contention, the actual SAW duration available for sensing decreases, hence, more sensing is missed. SAW duration 10 is too short for EDCA, so 100% sensing is always missed. Except for  $nSTA = 1$  none of the configurations can give 0% PSM, which is important for sensing application performance. For SAW duration = 10, even though PSM is

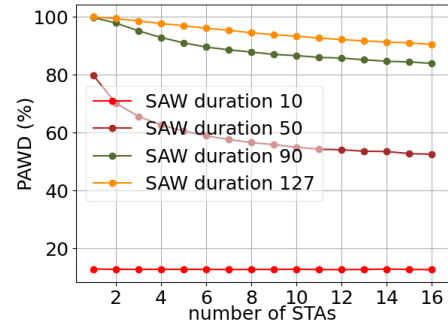
100%, there is overhead, which is due to partially missed sensing.

SAW duration 10 is too short even for PIFS access. Hence, 100% sensing is missed (see Fig. 4b). But SAW duration 90 and 127 give 0% throughput. Beyond  $nSTA = 9$ , SAW duration 50 is not long enough, to send all the sensing information bytes due to a decrease in RU size per STA.

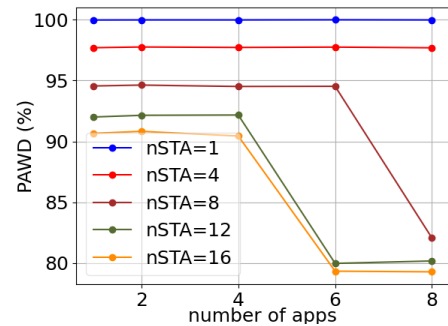
With EDCA access, from Fig. 5a, it can be seen that the throughput goes down when sensing is on (compared to no sensing). As  $nSTA$  increases, the throughput decreases due to more contention and collisions. Also, as SAW duration increases, the throughput decreases because more time is used for sensing. For SAW duration 10 and  $nSTA \geq 3$ , the throughput almost equals that of no sensing case because the actual available sensing duration becomes very short due to higher TxOP contention.

As shown in Fig. 5b, with PIFS access, the throughput is lower than the respective EDCA cases due to higher sensing overhead (and lower missed sensing). The throughput of SAW durations 50, 90, and 127 are almost equal since sensing overheads for these cases are nearly equal.

With EDCA access, PAWD generally decreases as  $nSTA$  increases due to an increase in contention (see Fig. 6a). As expected, the higher the SAW duration, the higher the PAWD. PAWD is always found to be 100% or very close to 100% for PIFS access (not shown in a graph).

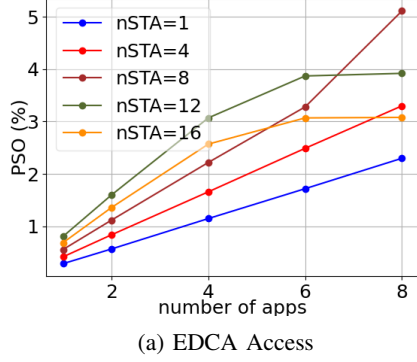


(a) Configuration 1

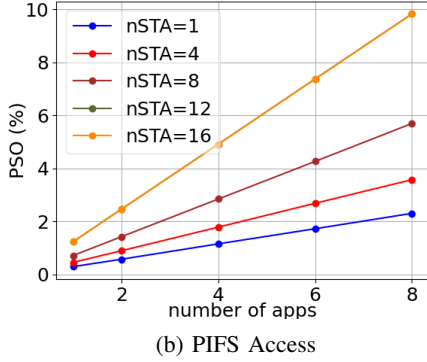


(b) Configuration 2

Fig. 6: Available Window Duration vs. number of STAs (EDCA Access)



(a) EDCA Access



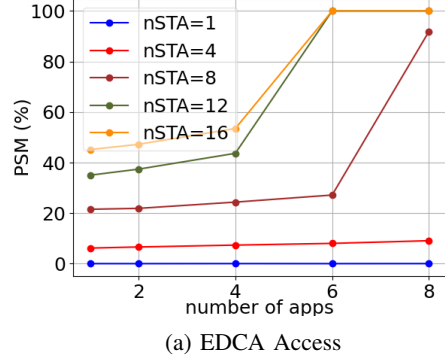
(b) PIFS Access

Fig. 7: Sensing Overhead vs number of Apps (Configuration 2)

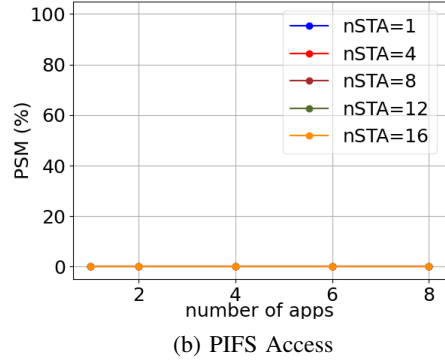
2) *Configuration 2*: With EDCA access, PSO generally increases as  $numApp$  increases (Fig. 7a). At high  $numApp$  (e.g., 6 and 8), for  $nSTA = 12$  and  $nSTA = 16$ , PSO remains flat, because the number sensing information bytes that can be sent in the SAW duration is limited by the RU size allocated to the STA. This can also be explained through PSM graph in Fig. 8a where between  $numApp = 6$  and 8, PSM becomes 100% for  $nSTA = 12$  and 16. We notice that the overhead of  $nSTA = 12$  is more than  $nSTA=16$ , which is counterintuitive. With  $nSTA = 16$ , there is less duration available for sensing due to more contention. Hence,  $nSTA = 12$  gets more sensing opportunities and incurs higher overhead. We also notice that for  $nSTA = 8$ , overhead goes beyond  $nSTA = 12$  and 16 at  $numApp = 8$ .  $nSTA = 8$  has a larger RU size than  $nSTA = 12$  and 16, and at  $numApp=8$  there are more sensing information bytes to be sent than at lower  $numApp$  values. Hence, more sensing information bytes could be sent at  $nSTA = 8$  than at  $nSTA = 12$  and 16.

In the case of PIFS access, overhead consistently increases as  $numApp$  increases and  $nSTA$  increases (see Fig. 7b). This can be explained by observing PSM (see Fig. 8b), where there is no sensing missed. Hence, overhead increases with an increase in  $numApp$  and also with an increase in  $nSTA$ .

Fig. 8a shows that with EDCA access, PSM increases as  $numApp$  increases. At some  $nSTA$  values, the jump is more drastic at certain  $numApp$ . For example, for  $nSTA = 12$  and 16, as  $numApp$  increases from 4 to 6, the report size increases



(a) EDCA Access



(b) PIFS Access

Fig. 8: Missed Sensing vs. number of Apps (Configuration 2)

such that with the allocated RUs, the full report cannot be sent even for one application. Hence, PSM increases drastically to 100%. For  $nSTA = 1$  and 4, the  $numApp$  increase does not affect PSM due to low report size.

In the case of PIFS access (see Fig. 8b), there is no missed sensing in any configuration since PIFS gives priority access to the channel and the SAW duration 127 is long enough to send all the sensing information bytes.

With EDCA access (see Fig. 9a), for a given  $nSTA$ , the throughput goes down slowly as  $numApp$  increases since it is only affected by the report size increase. But for a given  $numApp$ , as  $nSTA$  increases, the throughput drops much more due to higher contention and collisions as well as due to report size increase. For  $nSTA = 12$  and 16, as  $numApp$  increases from 6 to 8, the throughput remains flat because the PSO, in this case, does not change (see Fig. 7a).

From Fig. 9b, we observe that with PIFS access, the throughput decrease is steeper than EDCA access as  $numApp$  increases, since PIFS access incurs 0% PSM and higher sensing overhead than EDCA access.

Fig. 6b shows the PAWD performance for EDCA access. Since the SAW duration is 12.7 ms and TxOP is 5.484 ms, sensing can have up to three TxOPs. When  $nSTA$  is small (1 and 4), then increasing  $numApp$  does not change the duration and the number of TxOPs required to complete sensing. Hence, PAWD remains almost constant. But at large  $nSTA$  and large  $numApp$ , (e.g.,  $nSTA = 12$  and  $numApp = 6$ ), it requires more TxOPs to finish sensing operation. Since each TxOP is subject to contention, PAWD comes down. PAWD is always 100% or close to 100% for PIFS access (not shown).

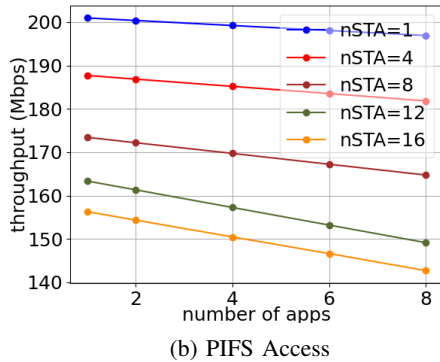
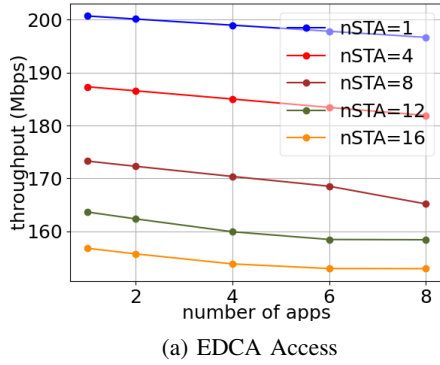


Fig. 9: Throughput vs. number of Apps (Configuration 2)

3) *Discussion*: From the above discussions on our simulation results, we highlight the following key points. Since keeping PSM to 0% is important for the performance of a sensing application, EDCA access is not a suitable option as it can lead to missed sensing in almost all cases. So, PIFS-based access should be used for sensing. Very short PAW duration (e.g., 10) is not a good choice, even at a very low sensing load, since it leads to missed sensing. In fact, with PIFS access, it is better to set the SAW duration to its maximum value 127 to avoid missed sensing. For this SAW duration value, the performance impact of sensing on data communication in terms of PSO and throughput is almost identical to smaller SAW durations for which there is no missed sensing. With PIFS access, when  $numApp = 4$  and  $nSTA = 16$ , the overhead is about 5% (see Fig. 3b) and the throughput drops by about 8 Mbps (or about 5%) compared to “no sensing” case (see Fig. 5b). Considering that this is a very high sensing load situation, the overhead and the throughput drop may be acceptable. Another important thing to note is that the RU size changes at discrete points (with respect to  $nSTA$ ), and there can be sudden changes in performance or performance may seem counterintuitive at those change points. These results also show that a system can be designed with an upper limit on sensing overhead. The AP in such a system would allow the sensing load to increase (by having more applications, stations, or more antennae) until the sensing overhead limit is reached.

## V. CONCLUSION

IEEE 802.11bf is a relatively new standard for Wi-Fi sensing. While integrating sensing with communication in a Wi-Fi

network leads to more efficient use of spectrum and hardware, it also contributes to communication overhead. Although the TGBf has carefully designed the IEEE 802.11bf protocol to limit the overhead, there is no sensing performance analysis of the protocol and its impact on data communication available in the literature. Hence, those are the focus of this paper. Our simulation results show that when NDPA sounding phase with reporting is enabled, EDCA access is not suitable for sensing, since it can lead to missed sensing. Also, a very short SAW duration (e.g., 10), even at a low sensing load, is not a good choice since it leads to missed sensing. A good rule of thumb is to have PIFS access with SAW duration set to a large value (e.g., its maximum value of 127), which ensures 0% PSO in almost all cases.

## REFERENCES

- [1] Y. Ma, G. Zhou, and S. Wang, “WiFi sensing with channel state information: A survey,” *ACM Computing Surveys (CSUR)*, vol. 52, no. 3, pp. 1–36, 2019.
- [2] H. Abdelnasser, K. A. Harras, and M. Youssef, “Ubbreath: A ubiquitous non-invasive wifi-based breathing estimator,” in *Proceedings of the 16th ACM international symposium on mobile ad hoc networking and computing*, 2015, pp. 277–286.
- [3] W. Li, R. J. Piechocki, K. Woodbridge, C. Tang, and K. Chetty, “Passive wifi radar for human sensing using a stand-alone access point,” *IEEE Transactions on Geoscience and Remote Sensing*, vol. 59, no. 3, pp. 1986–1998, 2020.
- [4] H. Abdelnasser, M. Youssef, and K. A. Harras, “Wigest: A ubiquitous wifi-based gesture recognition system,” in *2015 IEEE conference on computer communications (INFOCOM)*. IEEE, 2015, pp. 1472–1480.
- [5] S. Arshad, C. Feng, Y. Liu, Y. Hu, R. Yu, S. Zhou, and H. Li, “Wi-chase: A wifi based human activity recognition system for sensorless environments,” in *2017 IEEE 18th International Symposium on A World of Wireless, Mobile and Multimedia Networks (WoWMoM)*. IEEE, 2017, pp. 1–6.
- [6] S. Mosleh, J. B. Coder, C. G. Scully, K. Forsyth, and M. O. A. Kalaa, “Monitoring respiratory motion with Wi-Fi CSI: Characterizing performance and the BreatheSmart algorithm,” *IEEE Access*, pp. 1–1, 2022.
- [7] L. Storrer, H. C. Yildirim, M. Crauwels, E. I. P. Copa, S. Pollin, J. Louveaux, P. De Doncker, and F. Horlin, “Indoor tracking of multiple individuals with an 802.11ax Wi-Fi-based multi-antenna passive radar,” *IEEE Sensors Journal*, vol. 21, no. 18, pp. 20462–20474, 2021.
- [8] P. Falcone, F. Colone, A. Macera, and P. Lombardo, “Localization and tracking of moving targets with Wi-Fi-based passive radar,” in *2012 IEEE Radar Conference*, 2012, pp. 0705–0709.
- [9] “IEEE p802.11bf™/d3.0 draft standard for information technology—telecommunications and information exchange between systems local and metropolitan area networks— specific requirements part 11: Wireless LAN medium access control (MAC) and physical layer (PHY) specifications amendment 2: Enhancements for wireless LAN sensing,” 2023.
- [10] T. Ropitault, S. Blandino, A. Sahoo, and N. Golmie, “IEEE 802.11bf: Enabling the widespread adoption of wi-fi sensing,” accepted in *IEEE Communications Standards Magazine*: [https://tsapps.nist.gov/publication/get\\_pdf.cfm?pub\\_id=935175](https://tsapps.nist.gov/publication/get_pdf.cfm?pub_id=935175), [Online; accessed September 28, 2023].
- [11] S. Blandino, T. Ropitault, C. R. da Silva, A. Sahoo, and N. Golmie, “IEEE 802.11 bf DMG sensing: Enabling high-resolution mmwave wi-fi sensing,” *IEEE Open Journal of Vehicular Technology*, vol. 4, pp. 342–355, 2023.
- [12] “802.11ax lightsim,” <https://github.com/yousri-daldoul/802.11ax-lightsim>, accessed April 2023.
- [13] “Part 11: Wireless LAN Medium Access Control (MAC) and Physical Layer (PHY) Specifications,” 802.11 Working Group of the LAN/MAN Standards Committee of the IEEE Computer Society, Dec. 2020.
- [14] “IEEE p802.11az™/d7.0 draft standard for information technology—telecommunications and information exchange between systems local and metropolitan area networks— specific requirements part 11: Wireless LAN medium access control (MAC) and physical layer (PHY) specifications amendment 4: Enhancements for positioning sensing,” 2022.

- [15] Y. Daldoul, D.-E. Meddour, and A. Ksentini, "Performance evaluation of ofdma and mu-mimo in 802.11 ax networks," *Computer Networks*, vol. 182, p. 107477, 2020.